Les Cahiers du GERAD ISSN: 0711–2440

Optimizing stakeholders' objectives in a real-time multi-modal mobility hub system

A. A. Sadat Asl, H. Delmaire, A. Legrain, F. Soumis

G–2025–66

September 2025

La publication de ces rapports de recherche est rendue possible grâce au soutien de HEC Montréal, Polytechnique Montréal, Université McGill, Université du Québec à Montréal, ainsi que du Fonds de recherche du Québec – Nature et technologies.

Dépôt légal – Bibliothèque et Archives nationales du Québec, 2025
– Bibliothèque et Archives Canada, 2025

The publication of these research reports is made possible thanks to the support of HEC Montréal, Polytechnique Montréal, McGill University, Université du Québec à Montréal, as well as the Fonds de recherche du Québec – Nature et technologies.

Legal deposit – Bibliothèque et Archives nationales du Québec, 2025
– Library and Archives Canada, 2025

GERAD HEC Montréal
3000, chemin de la Côte-Sainte-Catherine
Montréal (Québec) Canada H3T 2A7

Tél. : 514 340-6053
Téléc. : 514 340-5665
info@gerad.ca
www.gerad.ca

Optimizing stakeholders' objectives in a real-time multi-modal mobility hub system

Ali Akbar Sadat Asl [a, b, c]

Hugues Delmaire [a]

Antoine Legrain [a, b, c]

François Soumis [a, b]

[a] *Department of Mathematical and Industrial Engineering, Polytechnique Montréal, Montréal (Qc), Canada, H3T 1J4*

[b] *GERAD, Montréal (Qc), Canada, H3T 2A7*

[c] *CIRRELT, Montréal (Qc), Canada, H3T 1J4*

ali-akbar.sadat-asl@polymtl.ca
hugues.delmaire@polymtl.ca
a.legrain@polymtl.ca
francois.soumis@polymtl.ca

September 2025
Les Cahiers du GERAD
G–2025–66

Abstract : Ridesharing could offer a solution to urban mobility challenges by delivering affordability and convenience while reducing congestion and environmental impact. This paper presents a system for multimodal mobility hubs with parking facilities, integrating personal vehicles with carpooling options and shuttle services into a cohesive network designed to accommodate real-time inbound and outbound ride requests. To address diverse interests and priorities within urban transportation, a column generation approach is employed to optimize the objectives of key stakeholders. An extensive computational study is performed using real-world public transit and ridesharing datasets from Québec City. The emission, user, and system objectives favor shared transportation options, while the operator objective shows a more substantial reliance on solo vehicles. Additionally, the results indicate that a transition to fully electric vehicles powered by a renewable energy mix can reduce average emissions by 78.1% compared to a scenario with gasoline-fueled vehicles. Rigorous evaluation across diverse scenarios demonstrates the proposed system's efficacy in addressing the complexities of large-scale transportation systems.

Keywords: Real-time ridesharing; column generation; multimodal transportation; mobility hub

Résumé : Le covoiturage pourrait constituer une solution aux défis de la mobilité urbaine en offrant à la fois accessibilité financière et commodité, tout en réduisant la congestion et l'impact environnemental. Cet article présente un système de pôles de mobilité multimodale avec des infrastructures de stationnement, intégrant les véhicules personnels, les options de covoiturage et les services de navette au sein d'un réseau cohérent conçu pour répondre en temps réel aux demandes de trajets entrants et sortants. Afin de tenir compte des divers intérêts et priorités en matière de transport urbain, une approche par génération de colonnes est utilisée pour optimiser les objectifs des principales parties prenantes. Une vaste étude computationnelle est réalisée à partir de jeux de données réels de transport en commun et de covoiturage provenant de la ville de Québec. Les objectifs liés aux émissions, aux usagers et au système favorisent les options de transport partagé, tandis que l'objectif de l'opérateur révèle une dépendance plus marquée aux véhicules individuels. De plus, les résultats indiquent qu'une transition vers un parc de véhicules entièrement électriques alimentés par un mix énergétique renouvelable pourrait réduire les émissions moyennes de 78.1% par rapport à un scénario basé sur des véhicules à essence. L'évaluation rigoureuse menée sur une diversité de scénarios démontre l'efficacité du système proposé pour relever la complexité des grands réseaux de transport.

Mots clés : Covoiturage en temps réel; génération de colonnes; transport multimodal; pôle de mobilité

1 Introduction

Urbanization and population growth are driving an increased reliance on personal vehicles. In 2021, 77.4% of work commutes in Canada were by car as a driver [1]. Furthermore, Canada had the sixth highest vehicle ownership rate globally in 2020, with 707 vehicles per 1,000 inhabitants [2]. Although personal vehicles provide convenience, they also exacerbate challenges related to urban planning, environmental sustainability, and social equity. To curb greenhouse gas emissions, the transition from internal combustion engine vehicles (ICEVs) to electric vehicles (EVs) is a key policy. By 2035, Canada aims to phase out the sale of ICEVs [3]. Leading this shift, EVs have seen remarkable growth, with nearly 185,000 new registrations in 2023—an increase of 49% from the previous year [4].

However, promoting public transportation remains a pivotal strategy to reduce environmental impacts and improve urban planning, traffic congestion, and social equity. Despite municipal efforts to encourage the use of public transit, one of the most persistent barriers to public transit adoption is the first- and last-mile problem—connecting commuters efficiently to and from transit hubs. This issue often imposes inconvenience and deters individuals from using public transportation. With the increasing popularity of ridesharing, there is growing recognition of the potential to integrate private and public transportation systems that can bridge this gap and enhance connectivity. There is thus an incentive for public transit authorities to leverage mobility innovations to facilitate collaboration between public and private sectors in ridesharing as shared transportation modes are likely to enhance the use of public transit [5].

Existing research on shared mobility systems primarily focuses on individual objectives or a combination of factors, often aiming for performance improvements from either an individual or operational perspective or a compromise that provides an overall satisfactory solution [6]. These approaches often fail to account for diverse stakeholders' priorities within a mobility system, leaving it unclear how emphasizing different objectives impacts operational demands and system behavior and dynamics. Furthermore, studies on integrating ridesharing with public transit have largely overlooked parking limitations at transit hubs, whereas parking constraints are a key factor in adopting ridesharing with personal vehicles [7].

To ensure the long-term viability of a shared mobility system, considering different objectives that reflect the diverse priorities of key stakeholders is critical. Users prioritize affordability, convenience, and travel time, while transportation companies (operators), as mobility service providers, focus on operational efficiency and profitability. Government agencies regulate transportation to reduce emissions and congestion while promoting sustainability and minimizing environmental impact. Meanwhile, society depends on a well-functioning system that fosters sustainability, equity, and public welfare while addressing critical urban challenges such as traffic congestion and infrastructure strain [8].

This paper highlights the critical role of ridesharing and proposes a system for multimodal mobility hubs equipped with parking facilities, addressing the objectives of key stakeholders, including user costs, operator expenses, emissions, and system-wide objectives. The proposed approach employs a Column Generation (CG) algorithm [9] to provide real-time assignments of requests to available vehicles while optimizing each stakeholder's objective separately to reveal how priority shifts influence the behavior of the mobility system. The system dynamically serves passengers traveling to the hub from their origins (inbound requests) and from the hub to their final destinations (outbound requests) within a public-private partnership framework. Public sector shuttle services and personal vehicles with carpooling options are considered as available transportation modes, each with distinct operational characteristics that affect overall system dynamics. Additionally, the impact of increased electrification on emissions reduction is evaluated by analyzing the transition from ICEVs to EVs.

The main contributions are summarized as follows:

- This paper introduces a multifaceted approach that independently optimizes the objectives of user, operator, emission, and overall system efficiency. The proposed method provides a de-

tailed depiction of the dynamic ridesharing ecosystem, analyzing system dynamics across various objectives to capture the diverse interests and priorities of key stakeholders.

- As a key feature of multimodal transportation hubs, parking capacity is integrated to accommodate personal vehicles, including those engaged in carpooling and solo vehicles heading toward the hubs. Given potential parking limitations, the system dynamically manages shuttle services alongside personal vehicles to optimize real-time transportation options.
- Using real-world data from Réseau de transport de la Capitale (RTC) in Québec, data instances are generated for empirical analysis to evaluate the potential of the proposed system across various scenarios. The dataset has been made publicly available to support further research. The findings offer actionable insights for policymakers and system designers to develop efficient and sustainable ridesharing frameworks.

The remainder of this paper is structured as follows: Section 2 reviews related studies on multimodal transportation and optimization algorithms in dynamic ridesharing. Section 3 describes the problem in detail. Section 4 presents the CG algorithm under different objectives. Section 5 discusses the implementation details and evaluates the performance of the proposed methodology through various case studies. Finally, Section 6 summarizes the key findings and offers recommendations for future research.

2 Related work

2.1 Multimodal transportation

Multimodal transportation involves using multiple modes of transportation within a unified system to facilitate passenger movement between various points. Multimodal transportation systems have gained increasing attention due to their potential to enhance sustainability, efficiency, and accessibility in urban mobility. Previous studies highlight trip planning and navigation services as an essential component of intelligent transportation systems [10, 11]. Understanding mode choice behavior in multimodal transportation is critical for designing efficient and sustainable systems. Studies in this field have explored the impact of different factors such as travel time, cost, and convenience on individuals' decisions across different transportation modes [12, 13].

Enhancing the accessibility and efficiency of multimodal transportation can be achieved by integrating public transit and ridesharing systems, promoting greater use of both, and contributing to more sustainable mobility [14]. Ma et al. (2019) proposed a ridesharing strategy that integrates transit services, allowing a private on-demand mobility service operator to drop off a passenger directly door-to-door, drop them off at a transit station, pick them up from a transit station or both pick up and drop off at two different stations using different vehicles. They designed queueing-theoretic algorithms based on an existing public transport system for vehicle dispatch and idle vehicle relocation. The objectives for request dispatching concern travel distance, passenger waiting and travel time. In this real-time operational context, the authors assumed no time window constraints for passenger requests [15].

Stiglic et al. (2018) examined the potential benefits of integrating ridesharing with public transit by proposing a centralized system to match drivers and riders. The transit service provider offers three match types: a ride-share match, where a driver transports a rider from origin to destination; a transit match, where a driver takes a rider to a transit station and then continues to their destination while the rider uses public transit; and a park-and-ride match, where the driver parks and uses public transport to reach their destination. The system maximizes matched passengers and drivers while minimizing extra trip duration. The ride-matching algorithm consists of a match identification phase and an optimization phase in which the optimal matching is determined based on the set of feasible matches with a branch-and-bound algorithm [16]

Significant research has explored multimodal transport systems, specifically addressing the first-mile/last-mile problem. These studies delve into how integrating various modes of transportation can effectively bridge the gap between the main transit stops and the initial and final legs of the trips to increase the accessibility and efficiency of transportation networks. Ma (2017) developed a dynamic algorithm for real-time dispatching and routing of ridesharing services in coordination with existing public transportation networks. The proposed algorithm groups requests based on shareability and finds optimal passengers-vehicles assignment to ensure bi-/multi modal trips. The algorithm first creates a pairwise request-vehicle graph to identify shareable rides, then computes a graph of feasible trips and the vehicles that can serve them before finally solving an integer linear program to match vehicles to trips to minimize the total waiting times and delays [17].

He et al. (2023) proposed a ridesharing approach for first-mile transportation to intercity transit hubs, formulating a mixed-integer linear programming model to minimize the cost for the ridesharing service operator while considering riders' requirements, including the latest arrival times, maximum ride times, large luggage, and travel time uncertainty. The system models a fleet of homogeneous passenger cars providing on-demand transportation for travelers who pre-book their rides. To solve the problem, the authors develop an adaptive large neighborhood search algorithm with an acceleration strategy and evaluate its solution quality using a column generation algorithm and a greedy heuristic [18].

Gu and Liang (2024) proposed a centralized transit system that integrates public transit and ridesharing, which matches drivers and transit riders so that the riders would have a shorter travel time using both transit and ridesharing. The system supports two match types: rideshare-transit, where a driver picks up multiple passengers from different origins and drops them at a single transit station, and transit-rideshare, where a driver picks up passengers from a transit station and drops them at multiple destinations. The optimization goal of the system is to maximize the number of riders assigned to ridesharing routes. The authors presented an exact approach (an integer linear program formulation based on a hypergraph representation) and approximation algorithms to achieve the optimization goal [19].

The proposed system in the present work considers public sector shuttle services and personal vehicles with carpooling options as available transportation modes, similar to the frameworks of Gu et al. (2024) and Stiglic et al. (2018), which also incorporate personal vehicles. However, parking availability is a crucial factor that significantly impacts the ridesharing decisions of personal vehicle owners. To address this challenge, this paper integrates parking capacity constraints and considers transportation hubs with limited dedicated parking spaces for personal vehicles heading toward the hubs, including those engaged in carpooling and solo vehicles. The proposed method dynamically manages shuttle services and personal vehicles, optimizing real-time transportation options and effectively utilizing hub parking spaces.

2.2 Optimization algorithms in dynamic ridesharing

Dynamic ridesharing is a special case of dynamic vehicle routing that aims to maximize car usage by pooling multiple passengers traveling to similar destinations into a shared ride. Optimizing ride matching, vehicle routing, and scheduling to minimize passenger waiting times, travel times, and vehicle operating costs remains a key challenge in dynamic ridesharing. Therefore, various optimization algorithms have been proposed in the literature, ranging from conventional mathematical programming approaches to heuristics and metaheuristics methods.

Herbawi and Weber (2012) proposed a genetic algorithm combined with an insertion heuristic to solve the dynamic ride-matching problem with time windows. Their multi-objective approach seeks to minimize the total travel distance and time for drivers, reduce riders' travel time, and maximize the number of matched requests. To handle the problem dynamically, they divided the day into time segments. At the start of each period, a genetic algorithm solves a static version of the problem using

all known requests and offers. Then, an insertion heuristic updates the solution in real-time as new requests or offers arrive until the period's end. Any unmatched requests or offers are stored and used as input for the genetic algorithm in the next period if they remain unmatched [20].

Alonso-Mora et al. (2017) proposed a reactive and scalable real-time method for assigning travel requests to a fleet of vehicles with varying capacities. The method returns an initial assignment of requests to vehicles and refines it over time, converging to an optimal solution. Their approach minimizes a cost function incorporating travel delay (drop-off time minus request time minus direct driving time) and a large constant for unassigned requests. When handling new requests, the algorithm first constructs a pairwise request-vehicle graph to identify potential shared rides. It then generates a graph of feasible trips and the vehicles capable of servicing them. Next, it solves an integer linear program, initialized with a greedy assignment, to allocate vehicles to trips. Finally, it repositions idle vehicles [21].

Simonetto et al. (2019) proposed a dynamic ridesharing algorithm based on federated optimization and a linear assignment problem. Their approach assigns batches of requests to available vehicles as follows: a central authority in the cloud collects requests and selects candidate vehicles based on their locations and seat occupancy. Then, the vehicles compute the cost of inserting each customer into their routes while satisfying customer constraints by solving a dial-a-ride problem. Next, they send these costs to the central server, and the cloud server optimally assigns requests to vehicles using a linear assignment problem based on the computed assignment costs. Finally, if some customers remain unserved, a reactive rebalancing phase is implemented with relaxed time constraints for idle vehicles only [22].

Cheikh-Graiet et al. (2020) developed a Tabu Search metaheuristic for dynamic carpooling, minimizing users' waiting time, delay, and trip cost while maximizing the gain in terms of CO2. Their proposed approach handles the transfer process and allows passengers to be dropped off at a designated walking distance from their destination or at a transfer node to improve user satisfaction. Additionally, the algorithm uses an aspiration process, the detour concept, to avoid getting trapped by local solutions and improve the generated solution. The algorithm uses the Choquet integral operator as an aggregation approach to account for the importance and interaction among the optimization criteria [23].

One approach that has garnered significant attention due to its ability to handle large-scale problems with multiple constraints and variables is Column Generation (CG). Applications of CG have shown promising results in dynamic ridesharing. Riley et al. (2019) studied the real-time dispatching of large-scale ridesharing services over a rolling horizon. They introduced a real-time dial-a-ride system that divides the time horizon into epochs and employs a CG approach to minimize wait times while ensuring service for every rider and limiting the deviation of each passenger's travel time from a direct trip. Additionally, the study proposes an optimization model that balances the minimization of waiting times with penalties for riders who have not yet been scheduled, ensuring that all riders are served within reasonable times. The penalties increase with each epoch, making it harder to neglect waiting riders [24].

Kim et al. (2022) studied a dynamic ridesharing problem and used a dynamic CG framework to maximize served requests while lowering passenger payments. The planning horizon is divided into epochs, each consisting of a CG phase and an optimization and implementation phase. In the CG phase, a restricted set-covering problem is iteratively solved, and the duals obtained are used to generate new feasible paths for active vehicles. The subproblem is the longest path variant of the elementary shortest path problem with resource constraints, solved using a labeling algorithm. This process continues within each epoch until a designated time limit is reached, allowing sufficient time to solve the integer program with the generated columns during the optimization and implementation phase [25].

While existing literature often focuses on improving performance from a specific perspective or finding a compromise solution among multiple criteria, this paper distinguishes itself by adopting a comprehensive approach to optimize the objectives of key stakeholders, including minimizing user costs, operator expenses, emissions, and vehicle underutilization as a system-wide objective. Considering parking limitations, this approach enables the analysis of system dynamics across various objectives, capturing stakeholders' diverse interests and priorities.

3 Problem description

3.1 Problem statement

This paper investigates the use of a transportation hub, which could be either the origin or destination of the trip. The transportation system is designed to serve the ride requests of passengers coming to a hub from their origins and those moving from the hub to their destinations. The hub is a centralized location where individuals can access many transportation modes. The system specifically considers personal vehicles with carpooling options alongside shuttles as dynamic transit solutions to serve ride requests. The hub has capacity constraints, including parking spots with varying costs, where different parking types are designated for personal vehicles engaged in carpooling and solo vehicles. Figure 1 illustrates a multimodal transportation system linking first- and last-mile mobility to urban transit networks. Riders can travel between their origins and the hub or from the hub to their destinations using shuttles or personal vehicles. Inbound personal vehicles can either go directly to the hub or pick up inbound riders along the way, while outbound personal vehicles can either go directly to their destinations or pick up outbound riders at the hub. The hub offers designated parking spots for arriving personal vehicles. From there, riders can transfer to transit services, which provide access to key urban areas such as the downtown core.

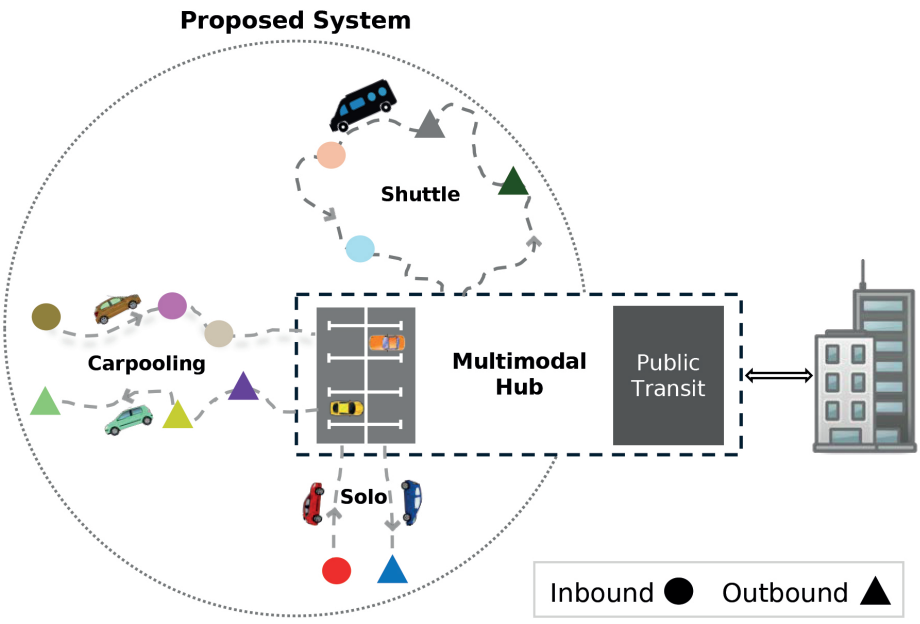

Figure 1: Proposed multimodal transportation system integrating first- and last-mile mobility and urban connectivity.

By incorporating capacity constraints, the system aims to provide real-time assignments of requests to available vehicles while separately optimizing each stakeholder's objective to understand the impact of priority shifts on the mobility system's dynamics and behavior. The emission objective aims to minimize the environmental impact associated with the life cycle emissions of shuttles and personal

vehicles, covering all stages from production to end-of-life disposal and recycling. The user cost objective for personal vehicles includes fuel consumption, maintenance, depreciation, parking fees, and user travel time, while for shuttles, it is driven solely by user travel time. From a user's perspective, shuttle costs exclude fuel, maintenance, and depreciation, as these expenses are borne by the operators. Shuttle operators aim to minimize expenditures on fuel, maintenance, depreciation, and driver wages while benefiting from governmental subsidies. For personal vehicles, operator costs are influenced by parking expenditures related to the maintenance of parking facilities. Lastly, the system-wide objective focuses on minimizing vehicle capacity underutilization to reduce congestion and improve traffic flow by ensuring vehicles are used to their fullest potential.

The following section presents a general mixed-integer programming (MIP) formulation that incorporates the constraints relevant to the abovementioned objectives. Building on this foundation, the CG approach is introduced, elaborating on the formulation and detailing how each objective contributes to the overall optimization model.

3.2 MIP formulation

The problem is defined by a fleet of vehicles, $\mathcal{V}$, a set of customers, $\mathcal{C}$, and a directed graph $\mathcal{G} = (\mathcal{N}, \mathcal{A})$. The graph consists of $|\mathcal{C}| + 2$ vertices, where the customers are denoted $1, 2, \ldots, n$, and the starting and returning hubs are represented by the vertices 0 and $n + 1$, respectively. The set of all vertices is denoted $\mathcal{N}$. Let $\mathcal{O}$ be the set of outbound nodes and $\mathcal{I}$ be the set of inbound nodes, where $\mathcal{C} = \mathcal{O} \cup \mathcal{I}$. The set of arcs, $\mathcal{A}$, represents direct connections between the hub and the customers and among the customers. With each arc (i, j), where $i \neq j$, a cost c_{ij} and a time t_{ij} are associated, which may include service time at customer i.

Each node i corresponds to a request, represented by $(o_i, d_i, m_i, r_i, a_i, b_i)$, where o_i and d_i denote the origin and destination of the trip, respectively, m_i represents the number of passengers, and r_i indicates the release time. Additionally, each customer is associated with a time window $[a_i, b_i]$, specifying the acceptable time frame for service provision, where $r_i \leq a_i \leq b_i$. A vehicle must arrive at the customer's location no later than the end of the time window, and if it arrives early, it must wait until a_i to commence servicing the customer.

Each vehicle k is characterized by $(b_k, l_k, q_k, s_k, e_k, h_k)$, where b_k and l_k indicate the vehicle's initial and final locations, q_k represents its capacity, s_k and e_k are its start and end times, respectively, and h_k denotes the vehicle's owner. Note that if $i = h_k$, then $o_i = b_k$ and $d_i = l_k$. Denote $\mathcal{V}_{out}$ as the set of personal vehicles departing from the hub ($b_k = 0$), $\mathcal{V}_{in}$ as the set of personal vehicles heading toward the hub ($l_k = n + 1$), and $\mathcal{V}_{shuttle}$ as the set of shuttle vehicles ($b_k = 0$ and $l_k = n + 1$). Then, $\mathcal{V} = \mathcal{V}_{shuttle} \cup \mathcal{V}_{out} \cup \mathcal{V}_{in}$. Two types of parking are considered: one designated specifically for carpooling and another shared among both carpooling and solo vehicles. Parking operators provide more flexibility to vehicles participating in carpooling, allowing them to park in both areas, whereas solo vehicles are restricted to the shared parking area. Accordingly, let t be the parking type, where $t \in \{carpool, shared\}$, with each parking type having a capacity γ_t. The cost of parking for vehicles participating in carpooling is β_c, while for solo vehicles, it is β_s.

The MIP model includes two sets of decision variables. The first variable, x_{ijk}, is binary and equals one if vehicle k travels directly from vertex i to vertex j. Shuttles first pick up outbound requests, drop them off, and then proceed to pick up inbound requests, whereas personal vehicles can serve outbound or inbound nodes. Consequently, $x_{ijk} = 0$ for all $i \in \mathcal{I}$, $j \in \mathcal{O}$, and $k \in \mathcal{V}$. The second decision variable, s_{ik}, is defined for each vertex i and each vehicle k. It represents the time at which vehicle k begins servicing customer i. A vehicle k can only start servicing requests after its start time and must reach its destination before its end time. Thus, $s_k \leq s_{ik} \leq e_k$ for all $i \in \mathcal{C}$ and $k \in \mathcal{V}$. Based on the above notation and assumptions, the static model is formulated as follows:

$$\min \sum_{k \in \mathcal{V}} \sum_{i \in \mathcal{N}} \sum_{j \in \mathcal{N}} c_{ij} x_{ijk} + \sum_{k \in \mathcal{V}_{in}} \sum_{i \in \mathcal{N}, i \neq b_k} \beta_c x_{i,n+1,k} + \sum_{k \in \mathcal{V}_{in}} \beta_s x_{b_k,n+1,k} \tag{1a}$$

$$\sum_{k\in\mathcal{V}}\sum_{j\in\mathcal{N}} x_{ijk} = 1 \qquad \forall i \in \mathcal{C}, \tag{1b}$$

$$\sum_{i\in\mathcal{N}}\sum_{j\in J} m_j x_{ijk} \leq I_k \qquad k \in \mathcal{V}, \tag{1c}$$

$$\sum_{j\in\mathcal{N}} x_{0jk} = 1 \qquad k \in \mathcal{V} \setminus \mathcal{V}_{in}, \tag{1d}$$

$$\sum_{j\in\mathcal{N}} x_{b_k,j,k} \leq 1 \qquad k \in \mathcal{V}_{in}, \tag{1e}$$

$$\sum_{i\in\mathcal{N}} x_{ipk} - \sum_{j\in\mathcal{N}} x_{pjk} = 0 \qquad p \in \mathcal{C}, p \neq h_k, k \in \mathcal{V}, \tag{1f}$$

$$\sum_{i\in\mathcal{N}} x_{i,l_k,k} = 1 \qquad k \in \mathcal{V} \setminus \mathcal{V}_{in}, \tag{1g}$$

$$\sum_{i\in\mathcal{N}} x_{i,l_k,k} = \sum_{j\in\mathcal{N}} x_{b_k,j,k} \qquad k \in \mathcal{V}_{in}, \tag{1h}$$

$$\sum_{i\in\mathcal{N}}\sum_{j\in\mathcal{O}} t_{ij} x_{ijk} \leq dev \cdot t_{0,l_k} \qquad k \in \mathcal{V}_{out}, \tag{1i}$$

$$\sum_{i\in\mathcal{N}}\sum_{j\in\mathcal{I}} t_{ij} x_{ijk} \leq dev \cdot t_{b_k,n+1} \qquad k \in \mathcal{V}_{in}, \tag{1j}$$

$$\sum_{k\in\mathcal{V}_{in}}\sum_{i\in\mathcal{N}} x_{i,n+1,k} \leq \gamma_{carpool} + \gamma_{shared}, \tag{1k}$$

$$\sum_{k\in\mathcal{V}_{in}} x_{b_k,n+1,k} \leq \gamma_{shared}, \tag{1l}$$

$$x_{ijk}\left(s_{ik} + t_{ij} - s_{jk}\right) \leq 0 \qquad i,j \in \mathcal{N}, k \in \mathcal{V}, \tag{1m}$$

$$a_j x_{ijk} \leq s_{0k} \qquad i \in \mathcal{N}, j \in \mathcal{O}, k \in \mathcal{V} \setminus \mathcal{V}_{in}, \tag{1n}$$

$$a_i \leq s_{ik} \leq b_i \qquad i \in \mathcal{I}, k \in \mathcal{V}, \tag{1o}$$

$$x_{ijk} \in \{0,1\} \qquad i,j \in \mathcal{N}, k \in \mathcal{V}. \tag{1p}$$

Equation (1a) minimizes the total travel and parking costs. Constraints (1b) ensure each customer is visited once; for customers that are final destinations of outbound vehicles, the condition is enforced on incoming arcs. Constraints (1c) state that a vehicle can only be loaded up to its capacity. More specifically, shuttles can transport outbound and inbound nodes up to their full capacity. Given a capacity limit of three for personal vehicles, those heading to the hub can pick up a maximum of two passengers in addition to the driver, totaling three occupants. Vehicles leaving the hub can deliver nodes up to their capacity. I_k can be, therefore, expressed as follows:

$$I_k = \begin{cases} q_k, & (k \in \mathcal{V}_{shuttle}, J = \mathcal{I}) \vee (k \in \mathcal{V} \setminus \mathcal{V}_{in}, J = \mathcal{O}), \\ q_k - 1, & (k \in \mathcal{V}_{in}, J = \mathcal{I}), \\ 0, & (k \in \mathcal{V}_{in}, J = \mathcal{O}) \vee (k \in \mathcal{V}_{out}, J = \mathcal{I}). \end{cases} \tag{2}$$

Constraints (1d)–(1h) require that each vehicle departs from the start location, leaves for another destination after servicing a customer, and finally, returns to the final location. That is, a vehicle $k \in V_{in}$ is required to reach its final destination only if it is used. To enhance the convenience of carpooling drivers, constraints can be introduced to set the maximum allowable travel time due to detours when accommodating carpooling passengers. This time is obtained by multiplying a deviation factor, *dev*, by the travel time of the direct path the driver would take if driving alone. Constraints (1i) and (1j) enforce this adjustment for both outbound and inbound personal vehicles, respectively. Constraints (1k) and (1l) are related to the capacity of different parking types. Constraints (1m) link the vehicle

departure time from a customer to its immediate successor. Furthermore, equations (1n) and (1o) ensure that the time windows are respected. Finally, constraints (1p) specify the permissible values of the decision variables. The next section will delve into the details of the CG algorithm, exploring the master and pricing problems across different stakeholders' objectives.

4 Methodology

The proposed framework employs a CG approach to dynamically manage shuttle services alongside personal vehicles to optimize real-time transportation options. CG divides the problem into smaller, more manageable subproblems, which can be solved independently and combined to find the optimal solution. Besides, it can dynamically generate new variables as the problem evolves over time, allowing for real-time optimization and adaptation to changing conditions. Finally, the CG approach is highly customizable, enabling the integration of additional constraints or objectives as needed.

The CG algorithm for integrating personal vehicles with carpooling options and shuttles begins by enumerating all possible columns for personal vehicles. These include direct columns, representing routes without detours or shared rides, and columns involving carpooling, which include routes with shared rides accommodating one or two passengers. These columns are initially added to the pool. The master problem is then solved to obtain dual values, which are subsequently used in $|\mathcal{V}_{shuttle}|$ independent subproblems formulated as resource-constrained shortest path problems. The subproblems apply the NG-path relaxation technique introduced by Baldacci et al. (2011) to generate new columns, which are then added back to the master problem [26]. This iterative process continues until no more columns with negative reduced costs can be identified, ensuring the overall solution is optimized. Upon completion of the column generation, the model solves a final MIP to impose integrality constraints on the master problem variables.

4.1 Master problem

This section presents the CG approach, beginning with the master problem. Let $\mathcal{P}_k$ represent the set of feasible paths for a given vehicle k. Specifically, for personal vehicles, the set of feasible paths can be defined as $\mathcal{P}_k = \mathcal{P}_k^1 \cup \mathcal{P}_k^2$, where $\mathcal{P}_k^1$ denotes the set of feasible carpooling columns for vehicle k, and $\mathcal{P}_k^2$ represents the single feasible non-shared column for vehicle k, which is the direct route from origin to destination. Moreover, α_{ip}^k denotes the number of times customer i is visited by vehicle k on path p. The model includes the following decision variables: y_p^k, which takes one if route p is selected for vehicle k, and c_p^k is the corresponding cost. In addition, w_i is defined as a penalty variable capturing if request i is not served and λ_i represents the associated cost. Table 1 summarizes the notations used in the CG algorithm.

This work aims to develop a comprehensive and integrated approach to urban mobility, providing real-time assignments of requests to available vehicles while minimizing different stakeholders' objectives. Therefore, the definition of c_p^k varies depending on each specific objective.

Emission: The emission objective minimizes the environmental impact caused by the life cycle emissions generated by shuttles and personal vehicles. In calculating life cycle emissions per kilometer, both operational and non-operational factors are taken into account. Operational emissions primarily come from fuel combustion or electricity consumption during vehicle use, while non-operational emissions, such as those from manufacturing and battery production (for EVs), are distributed per kilometer based on the vehicle's lifetime mileage. Let EM_p^k denote the emissions produced during travel on route p by vehicle k. Thus, the following holds:

$$c_p^k = EM_p^k, \qquad \forall k \in \mathcal{V} \tag{3}$$

User: For the user objective, c_p^k, for personal vehicles includes the costs of fuel consumption (FC_p^k), maintenance (MA_p^k), depreciation (DE_p^k), parking (PC_p^k), and travel time (TT_p^k) associated with route

Table 1: Sets, parameters, and variables of the CG algorithm

Master Problem	
Sets	
$\mathcal{V} = \mathcal{V}_{shuttle} \cup \mathcal{V}_{out} \cup \mathcal{V}_{in}$	Vehicles including shuttles, outbound and inbound personal vehicles
$\mathcal{C} = \mathcal{O} \cup \mathcal{I}$	Customers including outbound and inbound requests
$\mathcal{P}_k = \mathcal{P}_k^1 \cup \mathcal{P}_k^2$	Feasible columns (carpooling/non-carpooling) for vehicle k
Parameters	
c_p^k	Cost of path p for vehicle k
λ_i	Penalty for not serving request i
α_{ip}^k	Number of times customer i is visited by vehicle k on path p
γ_t	Capacity of parking type t
Variables	
y_p^k	1, if route p is selected for vehicle k
w_i	1, if request i is not served
Pricing Problem	
Sets	
$\mathcal{N}_k$	Set of vertices for vehicle k
$\mathcal{A}_k$	Set of arcs for vehicle k
Parameters	
c_{ij}	Cost of arc (i, j)
t_{ij}	Time of arc (i, j)
m_i	Demand of customer i
q_k	Capacity of vehicle k
$[a_i, b_i]$	Time window for request i
Variables	
x_{ijk}	1, if vehicle k drives directly from vertex i to j
s_{ik}	Time at which vehicle k serves vertex i

p and vehicle k, and measured in monetary units. In contrast, for shuttles, c_p^k is determined solely by the cost of travel time. Note that TT_p^k represents the cost of user travel time on path p by vehicle k, computed as the travel time multiplied by the Value of Time (VoT). A user's travel time is determined as the difference between a_i and their drop-off time. Moreover, the costs of FC_p^k, MA_p^k, and DE_p^k are calculated based on the kilometers traveled on a given path p. Similar to the emission objective, non-operational costs for personal vehicles, such as depreciation, are distributed per kilometer based on the vehicle's lifetime mileage.

$$c_p^k = \begin{cases} TT_p^k & \text{for } k \in \mathcal{V}_{shuttle} \\ FC_p^k + MA_p^k + DE_p^k + PC_p^k + TT_p^k & \text{for } k \in \mathcal{V} \setminus \mathcal{V}_{shuttle} \end{cases} \tag{4}$$

Operator: Under the operator objective, for the shuttles, c_p^k includes expenses related to fuel, maintenance, depreciation, and driver wages (DW_p^k). These costs are reduced by the governmental subsidies (GS_p^k) provided to the operator. For personal vehicles, c_p^k is determined by parking maintenance costs since other factors are not included due to vehicles' personal ownership. All shuttle-related costs are expressed per kilometer, and the distance traveled on a path determines the total cost of the path.

$$c_p^k = \begin{cases} FC_p^k + MA_p^k + DE_p^k + DW_p^k - GS_p^k & \text{for } k \in \mathcal{V}_{shuttle} \\ PC_p^k & \text{for } k \in \mathcal{V} \setminus \mathcal{V}_{shuttle} \end{cases} \tag{5}$$

System-wide: The system-wide objective prioritizes columns that minimize vehicle capacity underutilization. Let Q_k represent the vehicle capacity adjustment based on the vehicle type. Specifically, for shuttles capable of handling both outbound and inbound requests, $Q_k = 2q_k$, $k \in \mathcal{V}_{shuttle}$. For personal vehicles, which can handle either outbound or inbound nodes, $Q_k = q_k$, $k \in \mathcal{V} \setminus \mathcal{V}_{shuttle}$. Therefore, c_p^k

is defined as:

$$c_p^k = \frac{Q_k - \sum_{i \in \mathcal{C}} \alpha_{ip}^k}{Q_k}, \qquad \forall k \in \mathcal{V} \tag{6}$$

Based on the objectives outlined, the master problem is formulated as follows:

$$\min \sum_{k \in \mathcal{V}} \sum_{p \in \mathcal{P}_k} c_p^k y_p^k + \sum_{i \in \mathcal{C}} \lambda_i w_i \tag{7a}$$

$$\sum_{k \in \mathcal{V}} \sum_{p \in \mathcal{P}_k} \alpha_{ip}^k y_p^k + w_i = 1 \qquad \forall i \in \mathcal{C}, \qquad (\pi_i) \tag{7b}$$

$$\sum_{k \in \mathcal{V}_{in}} \sum_{p \in \mathcal{P}_k^1} y_p^k + \sum_{k \in \mathcal{V}_{in}} \sum_{p \in \mathcal{P}_k^2} y_p^k \leq \gamma_{carpool} + \gamma_{shared}, \tag{7c}$$

$$\sum_{k \in \mathcal{V}_{in}} \sum_{p \in \mathcal{P}_k^2} y_p^k \leq \gamma_{shared}, \tag{7d}$$

$$\sum_{p \in \mathcal{P}_k} y_p^k \leq 1 \qquad \forall k \in \mathcal{V}, \qquad (\sigma_k) \tag{7e}$$

$$y_p^k \geq 0 \qquad \forall k \in \mathcal{V}, \forall p \in \mathcal{P}_k, \tag{7f}$$

$$w_i \geq 0 \qquad \forall i \in \mathcal{C}. \tag{7g}$$

The objective function of the master problem minimizes the total travel costs and the penalties incurred by unserved riders, as expressed in (7a). Constraints (7b) make sure that each customer is visited only once, and if the request is not served, w_i is set to one to activate the penalty in the objective. Constraints (7c) and (7d) are associated with the parking capacity. Vehicles participating in carpooling can park in various types, while solo vehicles are limited to parking in the shared area. Constraints (7e) ensure that each vehicle is assigned to at most one column. Constraints (7f) and (7g) ensure that the decision variables are non-negative.

4.2 Pricing problem

The pricing problem is defined by a directed graph $\mathcal{G}_k = (\mathcal{N}_k, \mathcal{A}_k)$, $k \in \mathcal{V}_{shuttle}$. The routes for each shuttle are generated using a pricing problem designed to minimize the reduced cost associated with the variable y_p^k. This reduced cost is given by $c_p^k - \sum_{i \in C} \pi_i \alpha_{ip}^k - \sigma_k$, where π_i and σ_k are the dual variables corresponding to constraints (7b) and (7e), respectively. The objective function of the pricing problem varies depending on the objective and is given as follows:

Emission:

$$\boldsymbol{z}_k = \sum_{i \in \mathcal{N}_k} \sum_{j \in \mathcal{N}_k} (EM_{ij} - \pi_i) x_{ijk} - \sigma_k \tag{8}$$

User:

$$\boldsymbol{z}_k = \sum_{i \in \mathcal{O}} (s_{ik} - a_i - \pi_i) \sum_{j \in \mathcal{N}_k} x_{ijk} + \sum_{i \in \mathcal{I}} (s_{n+1,k} - a_i - \pi_i) \sum_{j \in \mathcal{N}_k} x_{ijk} - \sigma_k \tag{9}$$

Operator:

$$\boldsymbol{z}_k = \sum_{i \in \mathcal{N}_k} \sum_{j \in \mathcal{N}_k} (FC_{ij} + MA_{ij} + DE_{ij} + DW_{ij} - GS_{ij} - \pi_i) x_{ijk} - \sigma_k \tag{10}$$

System:

$$z_k = \sum_{i \in \mathcal{N}_k} \sum_{j \in \mathcal{N}_k} \left(\frac{-1}{Q_k} - \pi_i \right) x_{ijk} + 1 - \sigma_k \tag{11}$$

Shuttles first pick up outbound requests, drop them off, and then proceed to pick up inbound requests. Therefore, $\mathcal{A}_k$ excludes the direct edge from an inbound to an outbound request. A shuttle's departure time is determined by its arrival time at the hub and the ready times of the outbound requests it serves. The constraints of pricing problems include capacity constraints (1c), network constraints (1d)–(1g), time-related constraints (1m)–(1o), and the permissible values of the decision variables (1p).

5 Experimental evaluation

5.1 Instance description

The proposed approach is evaluated using data from RTC in Québec, where the on-demand service operates across several zones. This study focuses on the northwest zone, with the hub at Église Saint-Gérard-Majella. The RTC data on bus ridership includes the number of passengers boarding and alighting at various bus stops throughout the day. The number of outbound and inbound requests is determined by summing the alighting and boarding passengers at stops that provide access to the hub. The results are based on ridership data over ten weekdays in October 2019, with requests ranging from 436 to 702 during the simulation period. Besides, RTC provides on-demand transportation data from 2022-2023, including virtual stops and the distribution of the origins and destinations of the requests. The study area comprises 3155 virtual pick-up and drop-off points, enabling vehicles to serve customers without disrupting traffic. To encourage reproducibility and further research, the dataset is made openly accessible [27].

For outbound requests, the ready time is set to the arrival time of the alighting passengers, while for inbound requests, it is determined by subtracting the travel time to the hub and a random variability factor from the boarding time. The random factor (1–5 minutes) accounts for the variability in request preparation times. Requests are assumed to be released 15 minutes before their ready times. The simulation starts at 5:30 AM and runs until all requests with request times up to 6:45 PM are served, capturing morning and afternoon peak hours and mid-day demand. Re-optimization occurs every 15 minutes. Each inbound node is equipped with its own vehicle. For round trips, the system tracks whether an inbound request uses a personal vehicle, ensuring its availability for the return trip in the afternoon. For one-way outbound requests, it is assumed that less than 20% of users have their vehicles available. Furthermore, passengers are considered willing to participate in carpooling and comply with the system's decisions regarding vehicle assignments and routing.

In this work, personal ICEVs are assumed to be Honda Civics, while RTC shuttles are modeled as RAM ProMaster 2500s with a seven-passenger capacity. For the electrification scenarios, personal EVs are represented by Nissan Leafs, and electric shuttles are Toyota Proace Electric vans. The uniformity in vehicle type for users within the gas or electric categories enables more precise comparisons across objectives by removing variability that could arise from differing vehicle specifications. Moreover, emission parameters are sourced from Green NCAP [28], and vehicle operating costs are estimated using the Canadian Automobile Association's driving costs calculator [29]. Time is converted into monetary values based on Québec's minimum wage rate, with a VoT of $15 per hour.

5.2 Algorithmic and experimental setups

The master problem in the CG algorithm and the MIP model are solved using Gurobi 11.0.0. To solve the pricing subproblems, the cspy package [30] is used with the bidirectional labeling algorithm [31].

This work assesses how different configurations impact operational outcomes and system dynamics. For this analysis, six shuttles are initially deployed and 30 parking spots are allocated to each parking type ($S6P30$) as the base scenario. To examine the impact of shuttle availability and parking capacity on system performance, four additional scenarios are explored: $S6P20$ with six shuttles and 20 spots per type; $S6P\infty$ with six shuttles and sufficient spots per type (i.e., the number of each parking type is set large enough to ensure at least as many parking spaces as the maximum number of inbound vehicles over ten weekdays); $S3P30$ with three shuttles and 30 spots per type; and $S9P30$ with nine shuttles and 30 spots per type.

5.3 Re-optimization strategy

The system provides real-time assignments of requests to available vehicles capable of picking up customers within specified time constraints and without exceeding their seating capacity while minimizing the aforementioned objectives. Once routes are allocated to personal vehicles, they are then assigned fixed routes and are no longer available for new assignments. In contrast, shuttle routes remain adaptable and undergo dynamic adjustments throughout the optimization process. The system divides the time horizon into epochs of length ℓ, where each epoch τ corresponds to the time interval $[\tau\ell, (\tau+1)\ell)$. During epoch τ, while incoming requests are batched to be considered in the next epoch, the system optimizes the static problem using the requests accumulated in epoch $\tau-1$ and those not yet assigned in previous runs. This optimization is conducted over the interval $[(\tau+1)\ell, \infty)$.

To determine the starting stop for a shuttle, the optimization in epoch τ uses the solution of the static problem from epoch $\tau-1$ and considers the first stop within the interval $[(\tau+1)\ell, \infty)$ as b_k, with the earliest departure time for this stop provided by the solution from epoch $\tau-1$. Besides, the parking capacity parameter γ_t starts with an initial capacity and dynamically adjusts as vehicles depart and are allocated within the parking facility through optimization processes.

5.4 CG vs. MIP

Before performing a comparative analysis across the objectives, it is crucial to verify the effectiveness of the CG algorithm in real-time optimization. To achieve this, the results of the CG algorithm and the MIP model are compared. To generate instances for the offline comparison between the two approaches, simulations were conducted for a given day. The instances were selected randomly, with the condition that 60 to 70 percent of them fall within the morning and afternoon peak hours, and the remaining instances were allocated to other times of the day. This distribution provides a more comprehensive view of the methods' performance during peak and off-peak periods under various problem scales across different objectives.

The instances are named using a specific convention. The first letter denotes the objective ("O" for operator, "E" for emission, "S" for system-wide, and "U" for user objectives). The first number represents the instance, followed by the number of customers and vehicles. For example, "O1C53V48"refers to the first instance with 53 customers and 48 vehicles related to the operator objective.

Table 2 presents the comparative results, including the relative gap between MIP and CG (MC), calculated as $\frac{\text{MIP}-\text{CG}}{\text{CG}}$, along with the computational times and integrality gaps for both methods. For the MIP model, the time the best solution is first discovered and the total execution time, including the time to find the optimal solution and the time required to prove its optimality, are reported. A two-hour time limit is imposed on the total execution time, and the best solution found within this limit is recorded. The comparative analysis across various objectives reveals that the CG algorithm consistently outperforms MIP in solution quality and computational efficiency.

Under the operator objective, CG outperforms MIP in all cases, providing solutions that are, on average, 1.55% better than those from MIP. Moreover, CG achieves these results in an average of 48 seconds, compared to MIP's one-hour average total execution time. The integrality gap for CG is also

Table 2: Comparison of CG and MIP.

INSTANCE	MC (%)	TIME (Sec.)			INTEGRALITY GAP (%)	
		CG	MIP BEST-KNOWN	MIP TOTAL	CG	MIP
O1C53V48	3.17	45.16	6994	7200	2.34	30.64
O2C79V62	6.58	204.23	7200	7200	3.23	15.97
O3C58V37	0.18	83.98	1919	7200	5.02	9.31
O4C67V20	3.10	54.11	5855	7200	5.77	28.25
O5C32V17	0.00	49.30	53	94.42	3.37	0.00
O6C11V10	0.00	0.82	<1	0.75	0.00	0.00
O7C32V7	0.00	3.87	1	2.48	0.00	0.00
O8C55V16	2.48	38.80	6939	7200	3.11	31.20
O9C16V14	0.00	1.58	1	1.67	1.05	0.00
O10C24V27	0.00	0.87	2	2.63	0.00	0.00
AVERAGE	**1.55**	**48**	**2896**	**3610**	**2.39**	**11.54**
E1C53V48	1.90	21.88	6504	7200	1.13	51.09
E2C79V62	16.07	158.60	7020	7200	0.79	41.01
E3C58V37	10.74	105.71	6537	7200	0.75	22.11
E4C67V20	1.21	69.93	5917	7200	3.73	13.56
E5C32V17	0.00	33.51	132	1789.32	3.30	0.00
E6C11V10	0.00	0.83	<1	0.85	0.00	0.00
E7C32V7	0.00	3.14	1	3.29	0.00	0.00
E8C55V16	0.43	26.62	7195	7200	1.56	17.09
E9C16V14	0.00	1.85	3	3.77	1.05	0.00
E10C24V27	0.00	4.14	5729	7023.75	1.26	0.00
AVERAGE	**3.03**	**43**	**3904**	**4482**	**1.36**	**14.49**
S1C53V48	0.00	9.43	484	484.73	0.00	0.00
S2C79V62	0.00	32.94	4627	4627.92	0.00	0.00
S3C58V37	0.00	17.50	670	7200	8.33	25.00
S4C67V20	0.00	41.34	250	418.69	20.00	0.00
S5C32V17	0.00	74.52	7	257.06	21.58	0.00
S6C11V10	0.00	0.49	<1	0.18	0.00	0.00
S7C32V7	0.00	1.17	<1	0.49	29.27	0.00
S8C55V16	0.00	13.33	32	32.75	3.77	0.00
S9C16V14	0.00	1.73	<1	0.52	0.00	0.00
S10C24V27	0.00	3.88	22	1700.22	20.00	0.00
AVERAGE	**0.00**	**20**	**609**	**1472**	**10.30**	**2.50**
U1C53V48	107.81	10.23	6583	7200	0.26	123.95
U2C79V62	N/A	26.53	7187	7200	0.22	100.22
U3C58V37	56.07	135.69	7161	7200	2.09	90.15
U4C67V20	31.84	24.26	4261	7200	0.09	191.83
U5C32V17	4.29	20.25	6105	7200	0.34	71.39
U6C11V10	0.00	0.45	436	7195.57	0.26	0.00
U7C32V7	0.00	1.61	218	7200	0.00	97.26
U8C55V16	29.19	16.58	7183	7200	0.66	219.69
U9C16V14	1.42	2.04	373	7200	0.00	53.89
U10C24V27	9.66	0.96	1561	7200	0.11	176.24
AVERAGE*	**26.70**	**24**	**3765**	**7200**	**0.42**	**113.82**

*The average under the user objective is calculated by excluding U2C79V62, as the MIP was unable to find a feasible solution within the two-hour time limit.

approximately 9 percentage points (pp) lower than that of MIP. A similar trend is observed under the emission objective. MIP's solutions are, on average, 3% worse than CG's, while CG completes its computations in 43 seconds on average, compared to MIP's 4482 seconds. Furthermore, the integrality gap for MIP is about 13 pp higher than CG's.

Regarding the system-wide objective, CG reaches the optimal solution in all instances, with zero percent gap from MIP. Generally, MIP performs better with the system-wide objective than other objectives, finding optimal solutions in 609 seconds on average, with a total execution time of 1472

seconds. Except for the third case, MIP did not reach the time limit in any instance. However, CG exhibits the highest integrality gap under this objective, averaging 7.8 pp higher than MIP.

Under the user objective, CG demonstrates significant superiority in solution quality and computational efficiency across all instances. Despite consistently hitting the time limit in nearly all instances, the solutions MIP finds are still 26.7% worse than CG's. In the second instance, MIP failed to find a feasible solution within the time limit, whereas CG identified the optimal solution in just 26 seconds. Overall, CG achieves optimal solutions in an average of 24 seconds. The integrality gap further underscores this disparity, with CG averaging 0.42% compared to MIP's 113.82%.

5.5 Comparative analysis across objectives

To enable a clearer comparison of stakeholders' objectives, it is necessary to assess their impact on modal share distribution and parking utilization throughout the day. Figure 2 shows the distribution of passengers across modes and parking occupancy percentages under different objectives for the baseline scenario ($S6P30$).

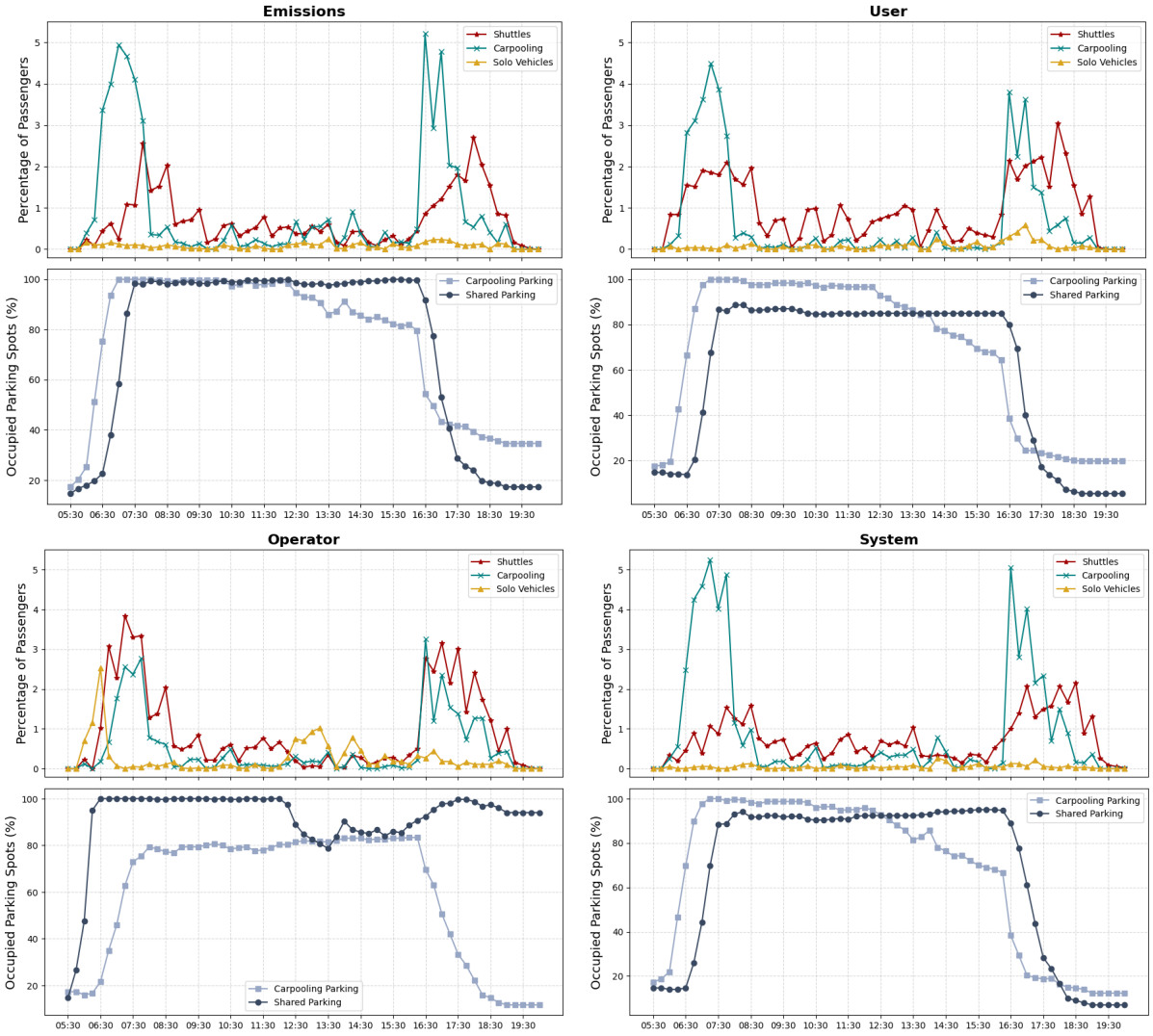

Figure 2: Average modal share and parking spot occupancy throughout the day for the baseline scenario (averaged over ten days).

Under the emission objective, carpooling reaches the highest modal share, sustaining 54.5% of the total passengers over the day. While shuttle use peaks at certain times, it remains lower than carpooling. Combined, carpooling and shuttles account for 95.3% of passengers, emphasizing reduced single-occupancy vehicles and promoting ridesharing. In contrast, the operator objective shifts toward increased solo vehicle use, with a 14.9% share throughout the day. Although this objective shows the lowest ridesharing adoption, it demonstrates a greater reliance on shuttles than carpooling during peak and off-peak hours.

The user objective favors shared modes, with carpooling significantly present during peak hours, similar to the emission objective. However, shuttle usage dominates throughout the day, accounting for 55.9% of passengers. This trend suggests a user-centered policy that minimizes individual costs and promotes shared modes, reaching 95.4% ridesharing across the day. The system objective achieves the highest ridesharing levels, with 54.9% of passengers using carpooling and 42.5% using shuttles, respectively. This prioritization reduces congestion and limits the number of empty vehicles, underscoring a focus on optimizing overall system efficiency.

Parking utilization peaks for carpooling and solo vehicles align with the high usage periods of these modes. As the day progresses, parking spaces that become vacant in the afternoon are reutilized. Specifically, under the emission, user, and system objectives, shared parking spaces are primarily occupied by vehicles engaged in carpooling, reflecting ridesharing priority in these objectives. Under the operator objective, however, solo vehicles primarily occupy shared parking. In the afternoon, as inbound requests—and thus parking demand—decrease, the percentage of occupied spots generally declines, except in shared parking under the operator objective, which remains nearly full, highlighting a stronger reliance on personal vehicle use.

5.5.1 Parking availability analysis

Reducing parking spaces ($S6P20$) decreases personal vehicle use, thereby increasing demand for shuttles, especially under the emissions and system-wide objectives. The emission objective sees an 18.2 percentage point (pp) drop in personal vehicle use (17.3 pp in carpooling, 0.9 pp in solo vehicles). Similarly, the system-wide objective shows an 18.2 pp decrease (17.2 pp in carpooling and 1.0 pp in solo vehicles) (see Figure 3). Conversely, increasing parking spots ($S6P\infty$) promotes greater use of personal vehicles, with carpooling rising 12.2 pp under emissions and solo vehicle use increasing 74.6 pp under the operator objective. Despite abundant parking options, the user and system objectives show greater resilience, with about a 5 pp increase in personal vehicle share each.

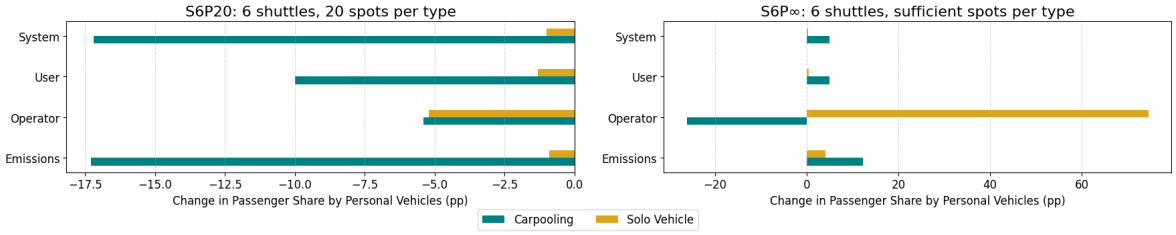

Figure 3: Shift in average personal vehicle share across parking scenarios compared to the baseline, measured in percentage points (averaged over ten days).

The analysis of each scenario compared to the baseline reveals distinct shifts in objectives based on parking and shuttle availability. In $S6P20$, there is an increase in all objectives, with the highest rise in user costs (21.4%), followed by operator (9.6%), system (6.7%), and emissions (4.9%), which suggests that reducing parking spots creates additional burdens, especially on user and operator objectives (see Figure 4). In contrast, $S6P\infty$ shows reductions across all objectives. Operator costs decrease by 80.3% due to improved solo vehicle feasibility, while emissions fall by 7.1% and system and user costs drop by 5.5% and 5.3%, respectively, thanks to increased carpooling.

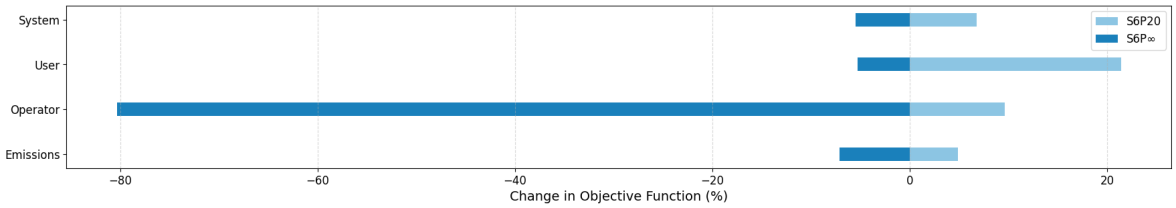

Figure 4: Percentage change in the average objective functions across parking scenarios compared to the baseline (averaged over ten days).

5.5.2 Shuttle availability analysis

Reducing the number of shuttles in $S3P30$ primarily affects the user and operator objectives, resulting in an 8.7 pp rise in personal vehicle usage for the user objective and a 7.0 pp increase for the operator objective (Figure 5). In contrast, increasing the number of shuttles ($S9P30$) leads to a 7.5 pp reduction in personal vehicle deployment under the user objective and a 8.9 pp decrease under the operator objective. The system and emission objectives exhibit smaller variations in passenger share across modes compared to the operator and user objectives when shuttle numbers change.

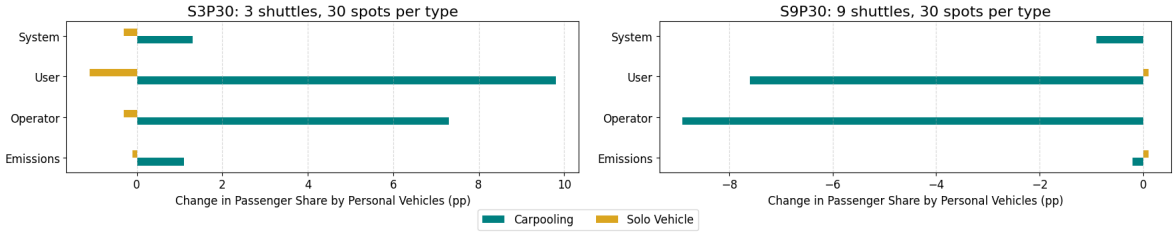

Figure 5: Shift in average personal vehicle share across shuttle scenarios compared to the baseline, measured in percentage points (averaged over ten days).

$S3P30$ significantly raises user costs by 75.1% due to longer travel times, while emissions, operator, and system costs are reduced, with system costs down by 9.8% (Figure 6). Lastly, $S9P30$ lowers user costs by 10.0% but results in a slight increase in emissions (0.9%) and a greater rise in system (1.2%) and operator costs (4.4%). This indicates that an expanded shuttle fleet can reduce user costs by improving service availability, though it comes with higher operator expenses and vehicle underutilization.

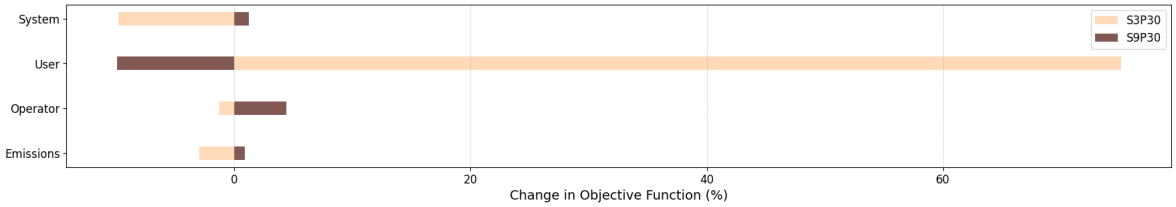

Figure 6: Percentage change in the average objective functions across shuttle scenarios compared to the baseline (averaged over ten days).

The following section explores the effects of transitioning from ICEVs to EVs under different scenarios, analyzing its impact on modal share and emissions reduction.

5.6 Electrification analysis

This section examines the transition from ICEVs to EVs, which can substantially reduce harmful emissions, as EVs do not rely on combustion engines. Moreover, while ICEVs incur higher fuel costs, EVs

experience greater depreciation, which balances out the financial differences for users and operators. The system-wide objective, which aims to minimize vehicle underutilization, remains dependent on vehicle capacity. Therefore, this section shifts focus to the environmental outcomes, examining how the transition to EVs directly impacts emissions and contributes to reducing the transportation sector's overall environmental footprint.

As of September 30, 2024, Québec has 337,854 EVs, representing approximately 5% of the total vehicles on the road [32]. The regional energy mix plays a key role in determining the life cycle emissions of EVs. Québec benefits from a predominantly renewable energy mix, with almost all of Hydro-Québec's electricity generated from renewable sources [33]. In contrast, regions like the U.S. rely heavily on fossil fuels, with more than 60% of electricity generation coming from nonrenewable sources [34].

To examine the environmental impact of electrification, different levels of EV adoption and energy sources are considered. Specifically, this analysis considers cases where 5% of personal vehicles are electric, reflecting the current adoption stage, and a fully electrified scenario in which all personal vehicles are EVs, representing a long-term future. Each case is evaluated under both renewable and nonrenewable energy mixes, resulting in four electrification scenarios: a nonrenewable mix with 5% personal EVs (N5PEV), a nonrenewable mix with 100% personal EVs (N100PEV), a renewable mix with 5% personal EVs (R5PEV), and a renewable mix with 100% personal EVs (R100PEV), with all shuttles being electric in each scenario. Figure 7 illustrates the average modal share across electrification scenarios compared to the baseline ($S6P30$).

In both energy mix scenarios, different levels of adoption show a reduction in personal vehicle share, indicating that replacing gasoline shuttles with electric ones encourages greater shuttle usage compared to the baseline. Both renewable and nonrenewable energy mixes exhibit similar behavior under varying levels of personal EV adoption. Specifically, as the adoption of personal EVs increases, there is less pressure on electric shuttle services, making personal vehicles a more justifiable choice, especially under a greener energy mix.

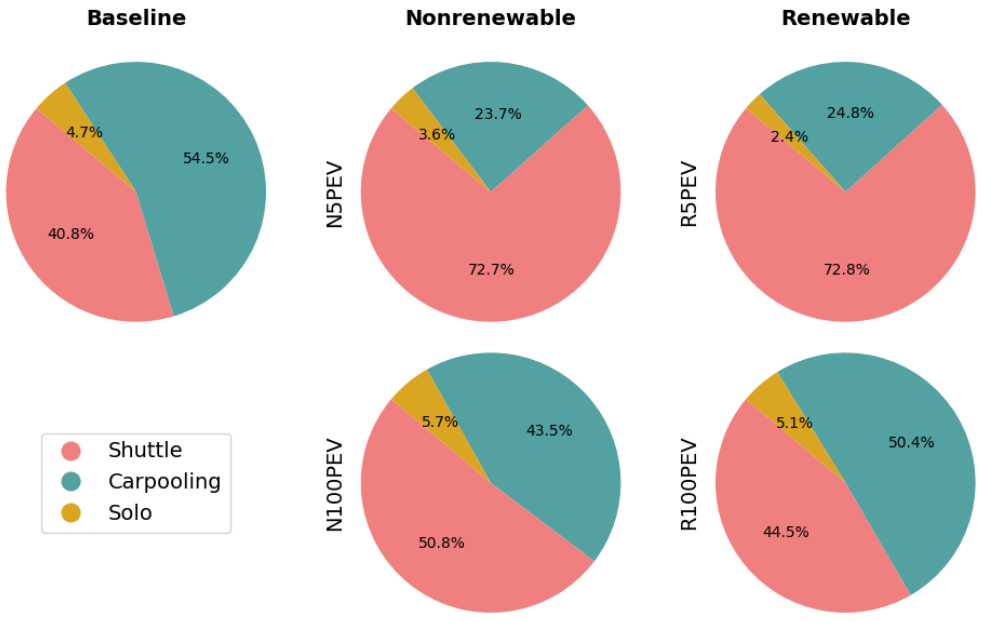

Figure 7: Average modal share across electrification scenarios compared to the baseline (averaged over ten days).

When comparing the renewable energy mix to the nonrenewable one at the same level of personal EV adoption, the renewable mix leads to greater ridesharing usage. In the nonrenewable 5 percent

adoption scenario (N5PEV), shuttle usage increases by 31.9 pp, while carpooling decreases by 30.8 pp, resulting in a 1.1 pp increase in ridesharing. Similarly, in the renewable 5 percent adoption scenario (R5PEV), personal vehicle use decreases by 32.0 pp, while ridesharing increases by 2.3 pp.

At full adoption of personal EVs, although solo vehicle usage increases slightly in both energy mixes, the renewable energy mix still encourages more ridesharing. Specifically, in the nonrenewable 100 percent adoption scenario (N100PEV), carpooling decreases by 11.0 pp, and solo vehicle usage increases by 1.0 pp. In the renewable 100 percent adoption scenario (R100PEV), the changes are a 4.1 pp decrease in carpooling and a 0.4 pp increase in solo vehicle usage.

The analysis of electrification scenarios relative to the baseline demonstrates varying emissions reductions based on the energy mix and the level of personal EV adoption. Figure 8 indicates the reduction in emissions in different electrification scenarios over ten weekdays.

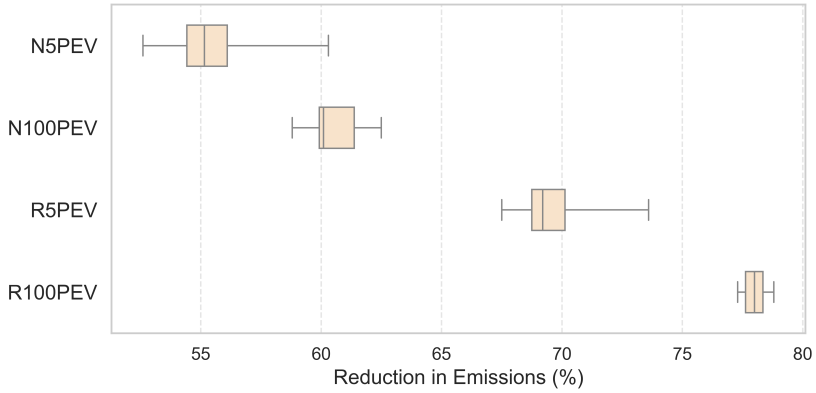

Figure 8: Impact of electrification on emissions reduction over ten days compared to the baseline.

For each energy mix, the higher adoption of personal EVs leads to a higher reduction in emissions. Under nonrenewable scenarios, N5PEV shows a reduction of between 52-60%, with an average of about 55.6%. With full adoption of personal EVs (N100PEV), the average reduction increases by 5.0 pp, reaching 60.6% compared to the baseline. In renewable scenarios, R5PEV achieves an emissions reduction between 67.5% and 73.6%, with an average of 69.7%. The R100PEV scenario results in the highest emissions reduction, averaging 78.1%, with minimal variation (77.3% to 78.8%). The renewable energy mix yields higher reductions than the nonrenewable mix. With 5 percent adoption of personal EVs, the greener energy mix leads to an average reduction that is 14.1 pp greater than with the nonrenewable mix, while full adoption results in an even greater reduction of 17.5 pp.

Overall, these findings reinforce the importance of resource planning to balance user convenience, environmental goals, operational costs, and system efficiency within urban mobility systems. By analyzing various scenarios, this work provides greater clarity on how prioritizing different objectives influences system dynamics and operational demands. Furthermore, by examining the impact of transitioning from ICEVs to EVs under both nonrenewable and renewable energy mixes across different electrification levels, this study can offer a clearer understanding of the future transportation landscape. These insights lay the groundwork for developing more adaptable, data-driven strategies that can guide future urban mobility policies and enhance the sustainability and efficiency of transportation systems.

6 Conclusion

This paper emphasized the integration of ridesharing solutions in urban transportation to tackle first- and last-mile challenges effectively. A CG algorithm was employed to optimize resource allocation among personal vehicles with carpooling options and shuttle services at multimodal mobility hubs,

revealing system dynamics and the interactions between these modes in shaping overall efficiency. The findings highlight how parking availability and shuttle capacity adjustments can shape modal share across user, operator, emission, and system-wide objectives. Each objective drives distinct modal behaviors, emphasizing specific trade-offs between reliance on solo vehicles and shared modes. The emissions, user, and system objectives favor shared transportation options. The operator objective, in contrast, shows a greater dependency on solo vehicles, highlighting potential challenges for reducing vehicle emissions and traffic congestion under operational cost-driven priorities.

While increasing shuttle numbers can reduce user costs and enhance service availability, it could lead to higher operator expenses. A demand-responsive shuttle allocation strategy can be implemented to adjust fleet size dynamically based on real-time ridership data. This strategy could involve predictive analytics to anticipate demand surges and flexible scheduling, where some vehicles are held in reserve and activated as needed, lowering operational costs while maintaining high service quality. Besides, sufficient parking availability enables carpooling to reach its full potential in supporting ridesharing, ultimately reducing costs across different objectives. However, excessive parking capacity could result in additional expenses when third parties provide parking spaces.

Analysis of the electrification scenarios indicates that the transition from ICEVs to EVs can reduce reliance on personal vehicles. Moreover, adopting EVs with a renewable energy mix leads to significantly higher emissions reductions than nonrenewable ones. The transition to electric shuttles, with the current adoption rate of personal EVs, could reduce emissions by up to about 70%, given Quebec's renewable energy mix. To support this shift, smart charging infrastructure should be integrated into multimodal mobility hubs to minimize operational downtime. Additionally, partnerships with local governments could facilitate incentive programs for EV adoption among personal vehicle users, further accelerating emissions reductions. Finally, understanding user preferences is crucial to better inform system design. Aligning transportation solutions with commuter expectations will enhance user satisfaction and promote the adoption of sustainable mobility options.

References

[1] Statistics Canada. (2022). Census: Main mode of commuting. Available at: https://doi.org/10.25318/9810045701-eng

[2] Organisation Internationale des Constructeurs d'Automobiles (OICA). (2020). Vehicles in Use. Available at: https://www.oica.net/category/vehicles-in-use

[3] Government of Canada (2023). Canada's Electric Vehicle Availability Standard: Regulated targets for zero-emission vehicles. Available at: https://www.canada.ca/en/environment-climate-change/news/2023/12/canadas-electric-vehicle-availability-standard-regulated-targets-for-zero-emission-vehicles.html

[4] Government of Canada (2024). Market Snapshot: Zero emission vehicles now account for over 10% of all new vehicles in Canada. Available at: https://www.cer-rec.gc.ca/en/data-analysis/energy-markets/market-snapshots

[5] Zuniga-Garcia, N., Gurumurthy, K. M., Yahia, C. N., Kockelman, K. M., & Machemehl, R. B. (2022). Integrating shared mobility services with public transit in areas of low demand. Journal of Public Transportation, 24, 100032.

[6] Martins, L.D.C., de la Torre, R., Corlu, C.G., Juan, A.A. and Masmoudi, M.A. (2021). Optimizing ride-sharing operations in smart sustainable cities: Challenges and the need for agile algorithms. Computers & Industrial Engineering, 153, p.107080.

[7] Haroon, W., Khan, M. A., Ilyas, Z., Almujibah, H. R., Zubair, M. U., Ashfaq, M., & Hamza, M. (2024). Analyzing Young Adult Travelers' Perception and Impacts of Carpooling on Traffic Sustainability. Sustainability, 16(14), 6098.

[8] Szmelter-Jarosz, A., & Rześny-Cieplińska, J. (2019). Priorities of urban transport system stakeholders according to crowd logistics solutions in city areas. A sustainability perspective. Sustainability, 12(1), 317.

[9] Desaulniers, G., Desrosiers, J. and Solomon, M.M. eds. (2006). Column Generation (Vol. 5). Springer Science & Business Media.

[10] Borole, N., Rout, D., Goel, N., Vedagiri, P. and Mathew, T.V. (2013). Multimodal public transit trip planner with real-time transit data. Procedia-Social and Behavioral Sciences, 104, pp.775-784.

[11] Li, J. Q., Zhou, K., Zhang, L., & Zhang, W. B. (2010). A multimodal trip planning system incorporating the park-and-ride mode and real-time traffic/transit information. In Proceedings ITS World Congress (Vol. 25, pp. 65–76).

[12] Habib, K.N. (2019). Mode choice modelling for hailable rides: An investigation of the competition of Uber with other modes by using an integrated non-compensatory choice model with probabilistic choice set formation. Transportation Research Part A: Policy and Practice, 129, pp.205-216.

[13] Azimi, G., Rahimi, A., Lee, M., & Jin, X. (2021). Mode choice behavior for access and egress connection to transit services. International Journal of Transportation Science and Technology, 10(2), 136–155.

[14] Zhang, Y., & Zhang, Y. (2018). Exploring the relationship between ridesharing and public transit use in the United States. International journal of environmental research and public health, 15(8), 1763.

[15] Ma, T. Y., Rasulkhani, S., Chow, J. Y., & Klein, S. (2019). A dynamic ridesharing dispatch and idle vehicle repositioning strategy with integrated transit transfers. Transportation Research Part E: Logistics and Transportation Review, 128, 417–442.

[16] Stiglic, M., Agatz, N., Savelsbergh, M. and Gradisar, M. (2018). Enhancing urban mobility: Integrating ride-sharing and public transit. Computers & Operations Research, 90, pp.12–21.

[17] Ma, T.Y. (2017). On-demand dynamic Bi-/multi-modal ride-sharing using optimal passenger-vehicle assignments. In 2017 IEEE International Conference on Environment and Electrical Engineering and 2017 IEEE Industrial and Commercial Power Systems Europe (EEEIC/I&CPS Europe) (pp. 1–5). IEEE.

[18] He, P., Jin, J. G., Schulte, F., & Trépanier, M. (2023). Optimizing first-mile ridesharing services to intercity transit hubs. Transportation Research Part C: Emerging Technologies, 150, 104082.

[19] Gu, Q.P. and Liang, J.L. (2024). Algorithms and computational study on a transportation system integrating public transit and ridesharing of personal vehicles. Computers & Operations Research, 164, p.106529.

[20] Herbawi, W.M. and Weber, M. (2012), July. A genetic and insertion heuristic algorithm for solving the dynamic ridematching problem with time windows. In Proceedings of the 14th Annual Conference on Genetic and Evolutionary Computation (pp. 385–392).

[21] Alonso-Mora, J., Samaranayake, S., Wallar, A., Frazzoli, E. and Rus, D. (2017). On-demand high-capacity ride-sharing via dynamic trip-vehicle assignment. Proceedings of the National Academy of Sciences, 114(3), pp.462–467.

[22] Simonetto, A., Monteil, J. and Gambella, C. (2019). Real-time city-scale ridesharing via linear assignment problems. Transportation Research Part C: Emerging Technologies, 101, pp.208–232.

[23] Cheikh-Graiet, S. B., Dotoli, M., & Hammadi, S. (2020). A Tabu Search based metaheuristic for dynamic carpooling optimization. Computers & Industrial Engineering, 140, 106217.

[24] Riley, C., Legrain, A. and Van Hentenryck, P. (2019). Column generation for real-time ride-sharing operations. In Integration of Constraint Programming, Artificial Intelligence, and Operations Research: 16th International Conference, CPAIOR 2019, Thessaloniki, Greece, June 4—7, 2019, Proceedings 16 (pp. 472–487). Springer International Publishing.

[25] Kim, M., Kim, H. and Moon, I. (2023). A column generation approach for a dynamic ridesharing problem. Transportation Letters, 15(9), pp.1114–1125.

[26] Baldacci, R., Mingozzi, A. and Roberti, R. (2011). New route relaxation and pricing strategies for the vehicle routing problem. Operations Research, 59(5), pp.1269–1283.

[27] Sadat Asl, A. A., Delmaire, H., Legrain, A., & Soumis, F. (2025). Dataset: Real-Time Multimodal Mobility Hub System [Data set]. Zenodo. https://doi.org/10.5281/zenodo.15122591

[28] Green NCAP. (2024). Life Cycle Assessment (LCA) Interactive Tool. Available at: https://www.greenncap.com/lca-tool

[29] Canadian Automobile Association (CAA)-Quebec. (2024). Vehicle driving costs. Available at: https://www.caaquebec.com/en/advices/tools-and-references/vehicle-driving-costs

[30] Sanchez, D.T. (2020). cspy: A Python package with a collection of algorithms for the (resource) constrained shortest path problem. Journal of Open Source Software, 5(49), p.1655.

[31] Tilk, C., Rothenbächer, A.K., Gschwind, T. and Irnich, S. (2017). Asymmetry matters: Dynamic halfway points in bidirectional labeling for solving shortest path problems with resource constraints faster. European Journal of Operational Research, 261(2), pp.530–539.

[32] Association des Véhicules Électriques du Québec (AVÉQ). (2024). Media / Information and Statistics. Available at: https://www.aveq.ca/meacutedias–stats.html

[33] Hydro-Québec. (2025). Our Energy. Available at: https://www.hydroquebec.com/about/our-energy.html

[34] U.S. Energy Information Administration (EIA). (2024). Electricity in the United States. Available at: https://www.eia.gov/energyexplained/electricity/electricity-in-the-us.php